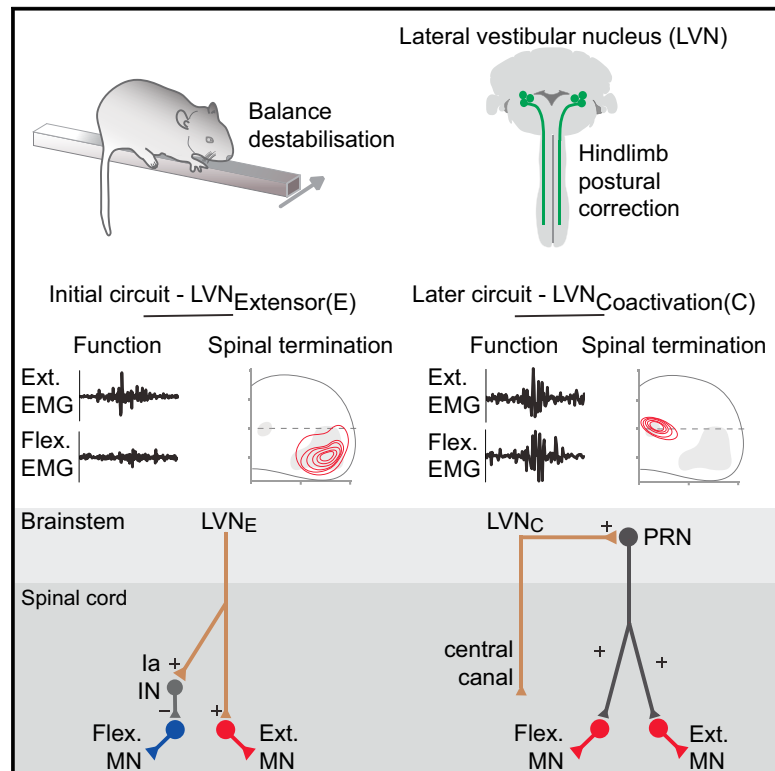


## Balance Control Mediated by Vestibular Circuits Directing Limb Extension or Antagonist Muscle Co-activation

### Graphical Abstract



### Authors

Andrew J. Murray, Katherine Croce, Timothy Belton, Turgay Akay, Thomas M. Jessell

### Correspondence

a.murray@ucl.ac.uk (A.J.M.), tmj1@columbia.edu (T.M.J.)

### In Brief

Murray et al. study how the nervous system generates an appropriate motor response following a postural perturbation. They identify two distinct cell types in the lateral vestibular nucleus that act together to maintain posture when a mouse undergoes a perturbation on a balance beam.

### Highlights

- Lateral vestibular nucleus (LVN) is required for fast responses to postural perturbation
- After perturbation, an early activated LVN cell type activates extensor motor neurons
- A later activated cell type generates a hind limb muscle co-contraction
- These non-overlapping cell types produce a coordinated response to balance perturbation



# Balance Control Mediated by Vestibular Circuits Directing Limb Extension or Antagonist Muscle Co-activation

Andrew J. Murray,<sup>1,3,\*</sup> Katherine Croce,<sup>1</sup> Timothy Belton,<sup>1</sup> Turgay Akay,<sup>2</sup> and Thomas M. Jessell<sup>1,4,\*</sup>

<sup>1</sup>Zuckerman Mind Brain Behavior Institute, Kavli Institute of Brain Science, Department of Neuroscience, Department of Biochemistry and Molecular Biophysics, and Howard Hughes Medical Institute, Columbia University, New York, NY, USA

<sup>2</sup>Department of Medical Neuroscience, Faculty of Medicine, Dalhousie University, Halifax, NS, Canada

<sup>3</sup>Sainsbury Wellcome Centre for Neural Circuits and Behaviour, University College London, London, UK

<sup>4</sup>Lead Contact

\*Correspondence: [a.murray@ucl.ac.uk](mailto:a.murray@ucl.ac.uk) (A.J.M.), [tmj1@columbia.edu](mailto:tmj1@columbia.edu) (T.M.J.)

<https://doi.org/10.1016/j.celrep.2018.01.009>

## SUMMARY

Maintaining balance after an external perturbation requires modification of ongoing motor plans and the selection of contextually appropriate muscle activation patterns that respect body and limb position. We have used the vestibular system to generate sensory-evoked transitions in motor programming. In the face of a rapid balance perturbation, the lateral vestibular nucleus (LVN) generates exclusive extensor muscle activation and selective early extension of the hindlimb, followed by the co-activation of extensor and flexor muscle groups. The temporal separation in EMG response to balance perturbation reflects two distinct cell types within the LVN that generate different phases of this motor program. Initially, an LVN<sub>extensor</sub> population directs an extension movement that reflects connections with extensor, but not flexor, motor neurons. A distinct LVN<sub>co-activation</sub> population initiates muscle co-activation via the pontine reticular nucleus. Thus, distinct circuits within the LVN generate different elements of a motor program involved in the maintenance of balance.

## INTRODUCTION

Animals have a remarkable ability to maintain balance and posture in the face of a variable external environment. In response to sudden postural disruption, animals modify ongoing motor programs and select new and contextually appropriate patterns of muscle activation that consider both internal and external constraints (Wilson and Melville Jones, 1979; Horak, 2009). Moreover, animals with a spinal cord transection do not generate corrective motor acts after balance perturbation (Chvatal et al., 2013), indicating a critical role for descending projections from the brain.

The medial and lateral vestibular nuclei give rise to descending spinal pathways that play a key role in the maintenance of balance (Horak, 2009). Patients with vestibular sensory disruption

exhibit altered patterns of muscle activation as they attempt to maintain balance and posture (Allum and Honegger, 2013; Honegger et al., 2013). Such changes involve the pattern of muscle activation and the incidence of antagonist muscle co-activation (Tang et al., 1998). The vestibular nuclei also receive a variety of somatosensory inputs (Pompeiano, 1972; McCall et al., 2016), which are required for postural control (Beloozerova et al., 2003). These findings support a view in which vestibular and somatosensory information instructs motor commands for posture and balance. Nevertheless, little is understood about the organizational logic of central circuits that control the transitions in motor pattern needed to maintain balance (Horak, 2009; Ting and McKay, 2007).

Vestibular circuits influence spinal motor programs via the actions of two distinct descending systems. Within the medulla, the medial vestibulospinal tract sends axons to cervical spinal levels and is involved in head stabilization (Goldberg and Cullen, 2011). In contrast, the lateral vestibulospinal tract projects to all spinal levels and forms connections with motor neurons and interneurons (Grillner et al., 1970, 1971; Basaldella et al., 2015). Descending systems of cortical and cerebellar origin are also thought to impose commands that generate appropriate responses to postural perturbation—both through direct engagement of spinal motor circuits and by recruiting brainstem relay centers (Canedo, 1997; Humphrey and Reed, 1983; Timmann and Horak, 1998; Jacobs and Horak, 2007).

We have explored how the neural circuitry of the mouse vestibular system initiates motor programs that maintain balance after postural perturbation. We created a balance beam destabilization task that requires descending input from the lateral vestibular nucleus (LVN) and reveals a bipartite hindlimb muscle activation pattern. From an initial state of limb muscle alternation, mice rapidly initiate exclusive extensor muscle activation and transition to a period of relative muscle quiescence, followed ~30 ms later by a state of co-activation of extensor and flexor muscles controlling hip, knee, and ankle joints. Selective ablation of spinally targeted LVN neurons attenuates both the early extensor and later co-activation phases of EMG bursting, indicating that transitions in hindlimb motor behavior depend on descending inputs that involve the LVN.

These transitions in motor strategy reflect the actions of at least two distinct sets of LVN neurons, which can be



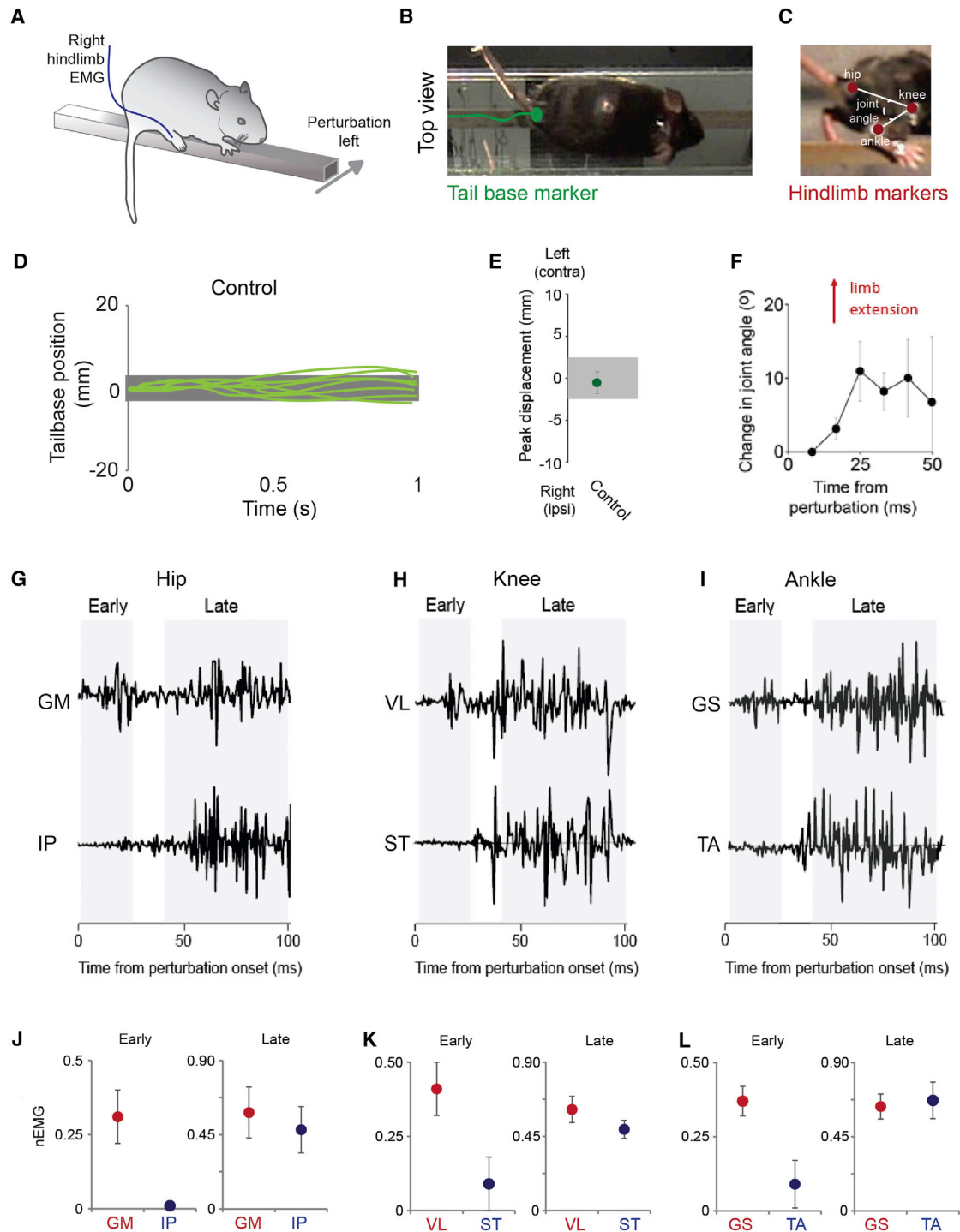


**Figure 1. Behavioral Assay to Switch from Antagonist Muscle Extension to Co-activation**

(A) Schematic of mouse walking on balance beam with right hindlimb EMG recording.  
 (B) Example image of reflective marker at the base of the tail, for kinematic analysis.  
 (C) Position of reflective markers at hip, knee, and ankle joints.  
 (D) Medial-lateral displacement of tail-base position after beam perturbation (time 0).  
 (E) Peak displacement of tail-base position.  
 (F) Joint angle at the knee after beam perturbation.  
 (G) Illustrative EMG signals from the hip muscles GM (extensor) and IP (flexor) after beam perturbation.

(legend continued on next page)

distinguished based on their output circuitry, timing of muscle activation, and motor function. An early-activated LVN set, termed  $LVN_E$  (extensor) neurons, forms direct contact with extensor, but not flexor, motor neurons and generate short latency limb extension without concurrent muscle co-activation. A second set, termed  $LVN_C$  (co-activation) neurons, terminates close to the central canal of the spinal cord and sends collaterals to the pontine reticular nucleus. Stimulation of  $LVN_C$  neurons co-activates flexor and extensor muscles without influencing earlier extensor responses. Together, these observations reveal distinctions in vestibular-activated brainstem and spinal circuits that generate a coordinated and contextually appropriate response to balance perturbation, providing an insight into how diverse neuronal subclasses within the LVN regulate balance.

## RESULTS

### Balance Perturbation Switches EMG Flexor-Extensor Activation Strategy

To elicit a postural response in adult mice, we combined a constrained base of support with an abrupt perturbation of the support surface. Animals were trained to walk on a balance beam 5 mm wide for 40 cm, from a defined start position to a darkened goal box located at the far end of the beam. Over a period of 1 week, animals gradually reached steady-state proficiency in balance performance, defined as regularly traversing the beam without stopping or foot slippage. A balance perturbation was then introduced by moving the beam rapidly (0.8 cm, 95 cm/s) to the animal's left, at variable positions in the latter half of the walk as mice advanced along a 10-cm length (Figure 1A). This sudden instability, combined with a narrow base of support, elicited a corrective motor reflex.

Kinematic responses to balance perturbation were monitored in the right hindlimb—the limb opposite to the direction of balance perturbation—and were captured using high-speed video as mice traversed the beam. Body and limb positions were monitored by placing reflective markers on the base of the tail and on the hip, knee, and ankle joints, permitting an estimate of the medio-lateral position of the body and approximate hindlimb joint angles (Akay et al., 2014; Figures 1B and 1C). In control mice, the tail-base position rarely extended beyond the bounds of the beam, an indication that animals compensated quickly for the leftward beam deflection (Figures 1D and 1E). Moreover, within 25 ms from the onset of perturbation, the knee angle subtended by the femur and tibia/fibula increased rapidly (Figure 1F), indicative of extension of the right hindlimb. The initial increase in joint angle plateaued as the hindlimb returned to the beam.

An electromyography (EMG) analysis of select muscles in the right hindlimb was performed over the first 100 ms after the onset of beam displacement. To enable within-animal comparison of EMG signals over different recording sessions, we normalized the EMG (normalized EMG; nEMG) signal to values obtained

with individual animals running on a treadmill at constant (0.3 m/s) velocity, immediately prior to beam walking (see [Experimental Procedures](#)). The area under the curve of the rectified EMG signal of a single muscle burst during one step cycle on the treadmill was assigned a reference value of 1, and EMG activation after beam perturbation is represented in relation to this value.

After beam displacement, an early activation phase, defined as a signal greater than 3 SD above the baseline value, with onset  $11 \pm 2$  ms (mean for all extensor muscles), was detected in three extensor muscles, the hip gluteus maximus (GM; nEMG =  $0.31 \pm 0.08$  relative to reference value [r.r.v.]), the knee vastus lateralis (VL; nEMG =  $0.4 \pm 0.09$  r.r.v.), and the ankle gastrocnemius (GS; nEMG =  $0.35 \pm 0.04$  r.r.v.) (Figures 1G–1L). In contrast, no EMG signal statistically different from zero was detected in the hip flexor iliopsoas (IP), knee flexor semitendinosus (ST), or ankle flexor tibialis anterior (TA) muscles (Figures 1G–1L). Over the next 10 to 20 ms, extensor activity declined to baseline, and little overt EMG activity was detected during this period. However, ~40–50 ms after beam displacement (mean =  $45 \pm 6$  ms), both extensor and flexor muscles at each joint were activated for a period of ~50 ms (Figures 1G–1L).

Thus, balance beam displacement induces a rapid transition in motor program. The initial phase is marked by exclusive activation of extensor muscles that arrests the step cycle over the period that the hindpaw returns to the balance beam. This extension was observed regardless of whether perturbation was applied during the swing or stance phases of the step cycle. There was, however, a tendency for the extension response to have a greater amplitude when perturbations were applied during swing phase, but this did not reach statistical significance (Figure S1). The early EMG phase was followed by an intervening quiescent phase and, finally, by a late phase in which extensor and flexor muscles are coactive, potentially to counteract ground impact forces or prevent joint rotation. The development of this behavioral assay permitted us to probe the neural circuitry that generates postural responses.

### LVN Neurons Are Required for Extensor Asymmetry and Antagonist Co-activation

To examine whether vestibular output circuits are involved in the beam-displacement-induced switch in motor strategy, we focused our attention on the LVN, the source of a conserved ipsilateral excitatory pathway to the lumbar spinal cord (Di Bonito et al., 2015; Liang et al., 2014; Wilson and Peterson, 1978). Mammalian LVN neurons receive direct vestibular sensory input from otolith organs and the posterior semicircular canal (Uchino et al., 2005; Zampieri et al., 2014).

Since the functional role of the LVN in balance control remains poorly defined (Di Bonito et al., 2015), we examined whether this nucleus underlies the switch in EMG response elicited by balance beam displacement. We examined behavioral and EMG responses when LVN neurons, defined by their lumbar

(H) Illustrative EMG signals at the knee muscles VL (extensor) and ST (flexor) after perturbation.

(I) Illustrative EMG signals at the ankle muscles: GS (extensor) and TA (flexor) after beam perturbation.

(J–L) Normalized EMG activity in the (J) hip, (K) knee, and (L) ankle extensor and flexor muscles after perturbation (n = 8 animals).

Data presented as mean  $\pm$  SEM.

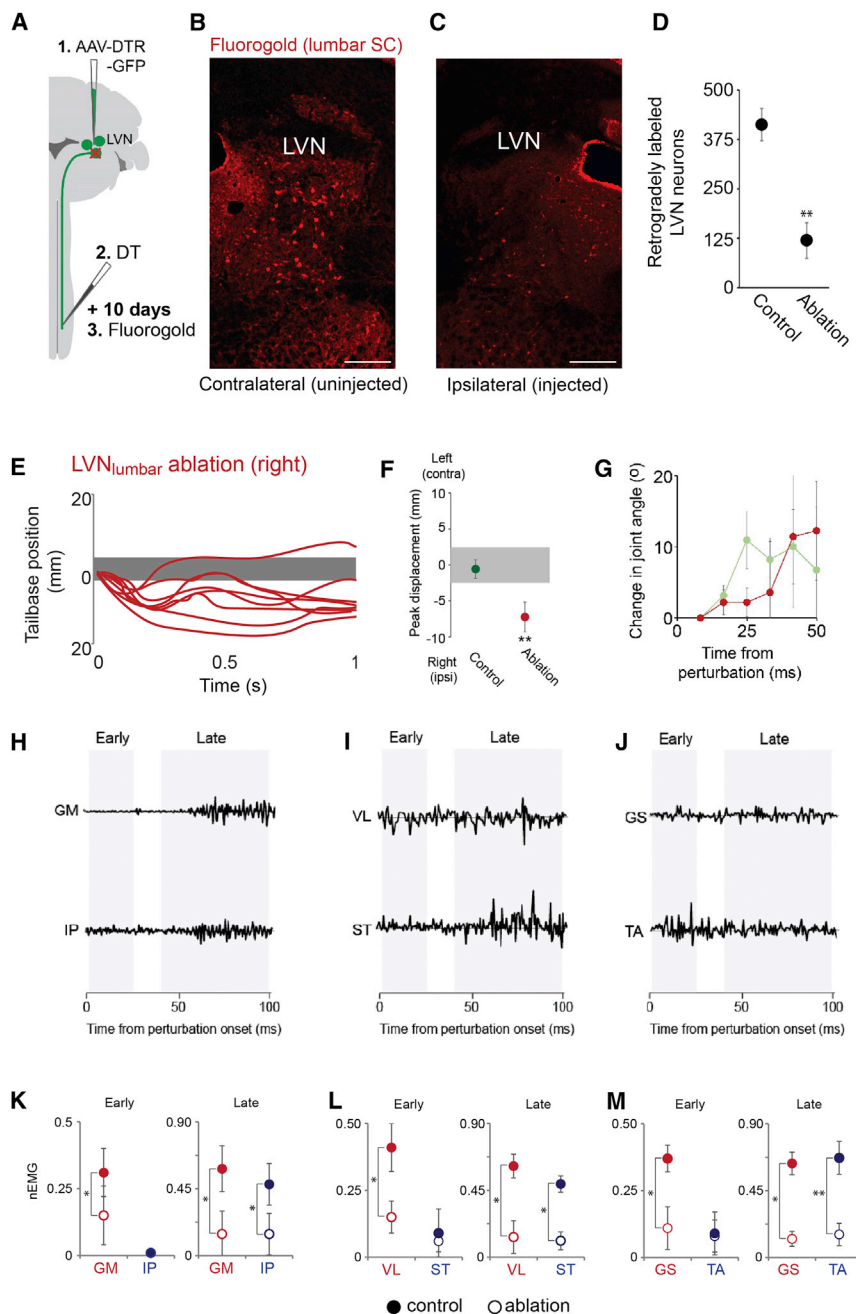


**Figure 2. Balance Impairment after Ablation of Lumbar-Projecting LVN Neurons**

(A) Strategy for selective ablation of lumbar-projecting LVN neurons.

(B and C) Fluorogold retrograde labeling of lumbar-projecting LVN neurons in the (B) ipsilateral (injected) and contralateral (uninjected) (C) LVN after DTR ablation.

(D) Quantitation of neurons in the LVN under control (no diphtheria toxin injection) and ablated conditions.

(E) Tail-base position after beam perturbation (time 0) following right lumbar LVN ablation.

(F) Quantitation of mean displacement of tail base after beam perturbation.

(G) Angle of the right knee after beam perturbation.

(H) Illustrative EMG signals at the hip muscles GM (extensor) and IP (flexor) after perturbation.

(I) Illustrative EMG signals at the knee muscles VL (extensor) and ST (flexor) after perturbation.

(J) Illustrative EMG signals at the ankle muscles GS (extensor) and TA (flexor) after perturbation.

(K–M) Normalized EMG activity in the (K) hip, (L) knee, and (M) ankle extensor and flexor muscles after perturbation with right lumbar LVN ablation (n = 8 animals).

Scale bars in (B) and (C), 250  $\mu$ m. Data are presented as mean  $\pm$  SEM in (D) and as mean  $\pm$  SD in (K)–(M). Error bars in (K) (IP Early) are not visible due to small size. \*p < 0.05; \*\*p < 0.01.

neurons to cervical spinal cord (Figure S2), an indication that other LVN-derived spinal and reticular projections are preserved (Boyle et al., 2004; Sarkisian, 2000).

In the open field, mice with lumbar LVN neuronal ablation exhibited no overt vestibular phenotype. We detected no circling movements or head bobbing, and mice retained a normal righting reflex (Hardisty-Hughes et al., 2010). Moreover after DT injection, analysis of kinematic and EMG patterns during treadmill running (Akay et al., 2014) failed to reveal overt differences to the normal locomotor pattern (Figure S3; n = 6 animals), although we did note a small increase in variance between lesioned and control groups (Figure S3). Additional analysis of

projections and nuclear position, had been eliminated (Liang et al., 2014). To obtain lesion selectivity, we first injected an adeno-associated virus (AAV) encoding the diphtheria toxin receptor (DTR) in the right LVN. 21 days later, we locally injected diphtheria toxin (DT) into the right side of the L3 segment of the spinal cord (Figure 2A; Figure S2). After a further 7 days, fluorogold (FG) was injected into L3 spinal cord to assess the residual LVN neuronal number (Figures 2B–2D). This strategy led to a  $68 \pm 4\%$  reduction in the number of lumbar-projecting LVN neurons (p = 0.001; n = 6 animals) (Figures 2B–2D). By comparison, we observed no noticeable reduction in the projection of LVN

treadmill walking at 0.3 m/s showed that there was no alteration in the phase of the step cycle following ablation or degradation in EMG recordings over time (Figure S3). Mice with lumbar LVN neuronal ablation exhibited a marked defect in their ability to correct for displacement of the balance beam. After balance perturbation in LVN-lesioned animals, the position of the tail base extended  $3.5 \pm 1.2$  mm beyond the bounds of the balance beam (Figures 2E and 2F; p = 0.0019, compared to control). We also observed that LVN-ablated mice traversed the balance beam at a slightly slower ( $\sim 10\%$ ) speed than control animals. In addition, the right hindlimb extensor movement was delayed

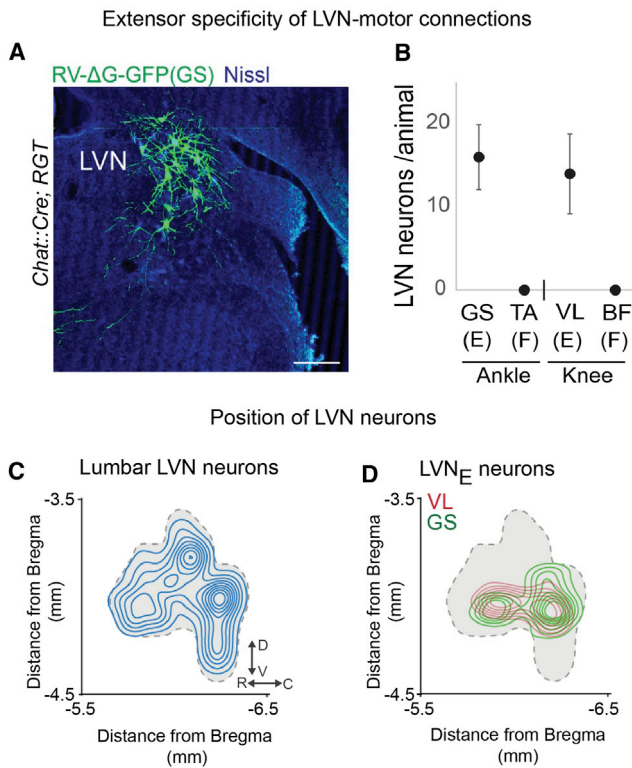


**Figure 3. Extensor, but Not Flexor, Motor Neurons Receive Mono-synaptic Input from the LVN**

(A) Image in the LVN after SAD-B19ΔG rabies virus into the GS muscles, with G protein complementation in motor neurons.  
 (B) Quantitation of LVN neurons infected with rabies virus after monosynaptic transfer from extensor or flexor motor neurons.  
 (C) Contour density plot showing a condensed sagittal projection through the ipsilateral LVN (gray area) and the position of lumbar LVN neurons, as assayed by fluorogold injection into spinal cord level L3.  
 (D) Contour density plot showing a condensed sagittal projection through the LVN and the position of LVN neurons connected mono-synaptically to motor neurons.  
 D, dorsal; V, ventral; R, rostral; C, caudal; E, extensor; F, flexor. Scale bar in (A), 400 μm. Data in (B) presented as mean ± SEM.

by  $15 \pm 2$  ms after LVN ablation compared to controls (one-tailed *t* test at the time when joint angle is significantly  $>0$ ; Figure 2G). The delay, rather than blockade of extensor activation, could imply either the recruitment of alternate descending or spinal systems or the activation of the remaining lumbar-projecting LVN neurons.

Analysis of hindlimb EMG activity after balance beam perturbation revealed that the ablation of lumbar LVN neurons elicited a significant attenuation of both early- and late-phase muscle EMG bursts (Figures 2H–2M). Quantitation of the EMG signal revealed a 60%–70% reduction in the early extensor exclusive phase of GS, VL, and GM muscles ( $n = 6$  animals; percent reductions in EMG signal: GS,  $71.2\% \pm 6.8\%$ ,  $p = 0.0001$ ; VL,  $65.2\% \pm 8.9\%$ ,  $p = 0.0001$ ; GM,  $60.3\% \pm 23.4\%$ ,  $p = 0.005$ ; all means ± SD) and a 60%–80% attenuation of the late-phase co-activation of these extensors, as well as their antagonistic TA, ST, and IP flexor muscles (Figures 2K–2M; percent reductions in EMG

signal: GM,  $70.9\% \pm 22.0\%$ ,  $p = 0.00022$ ; IP,  $66.6\% \pm 21.7\%$ ,  $p = 0.0003$ ; VL,  $78.3\% \pm 9.1\%$ ,  $p = 0.0001$ ; ST,  $77.3\% \pm 1.4\%$ ,  $p = 0.0001$ ; GS,  $81.1\% \pm 9.8\%$ ,  $p = 0.0001$ ; TA,  $77.2\% \pm 8.9\%$ ,  $p = 0.0001$ ; all means ± SD). In ~10% of trials in LVN-ablated animals, we also detected a small increase in early-phase flexor activity, consistent with a reduction in LVN-mediated reciprocal inhibition of flexor motor neuron activity (Grillner et al., 1971), but this did not reach statistical significance. Taken together, these findings indicate that spinally projecting LVN neurons are needed to elicit balance-induced motor programs, which impacts both the extensor exclusive and antagonist co-activation phases.

One potential mechanism for the generation of temporally separable phases of muscle activation in response to balance beam perturbation is the existence of separate LVN neuronal subclasses, with distinct activation features and output circuitry. Based on the EMG signal, we explored two potential LVN classes: one class (LVN<sub>E</sub> neurons) assigned to the selective activation of extensor muscles and a second class (LVN<sub>C</sub> neurons) tasked with the late-phase co-activation of flexor and extensor muscles. The existence of these two classes would be consistent with the suggested heterogeneity of cell types within the LVN, as assessed by the diversity in cell body and axon diameter of LVN neurons and varied physiological response properties (Pompeiano, 1991; Shinoda et al., 1986).

### LVN<sub>E</sub> Neurons Selectively Innervate Extensor Motor Pools

We first examined how the initial phase of extensor muscle activation in response to balance perturbation is achieved. To address this issue, we examined the output of LVN<sub>E</sub> neurons anatomically, assessing the labeling of neurons in the LVN after retrograde *trans*-synaptic transfer from defined motor pools using the glycoprotein deficient SAD-B19 rabies virus strain complemented with a mouse line that expresses rabies glycoprotein in motor neurons (*ChAT-Cre::RGT* mice) (Takatoh et al., 2013; Zampieri et al., 2014). We detected GFP-labeled LVN neurons (range = 12–21 ipsilateral neurons) after RABV-ΔG-GFP injection into GS or VL extensor muscles ( $n = 8$  animals) (Figure 3A), an indication that extensor motor pools receive direct LVN synaptic input. In contrast LVN neurons were not labeled after equivalent injections into the TA and biceps femoris (BF) flexor muscles (Figure 3B). Nevertheless, *trans*-synaptically traced neurons were observed in the pontine reticular nucleus (PRN) and other brainstem nuclei (data not shown), arguing for selectivity in innervation of extensor motor neurons by LVN neurons (Grillner et al., 1971).

To confirm the extensor specificity of LVN neurons, we performed orthograde tracing of the synaptic connections between LVN neurons and motor neurons, injecting an AAV construct encoding myristoylated GFP into the LVN, while monitoring colabeling of synaptic terminals with the vesicle-associated protein synaptophysin. We found that ~80% of GS extensor and ~60% of VL extensor motor neurons received input from GFP<sup>+</sup> LVN neurons, defined as  $>3$  GFP<sup>+</sup> synaptophysin<sup>+</sup> terminals contacting individual motor neuron dendrites (Figure S4). In contrast, the flexor TA and BF pools were devoid of direct LVN inputs

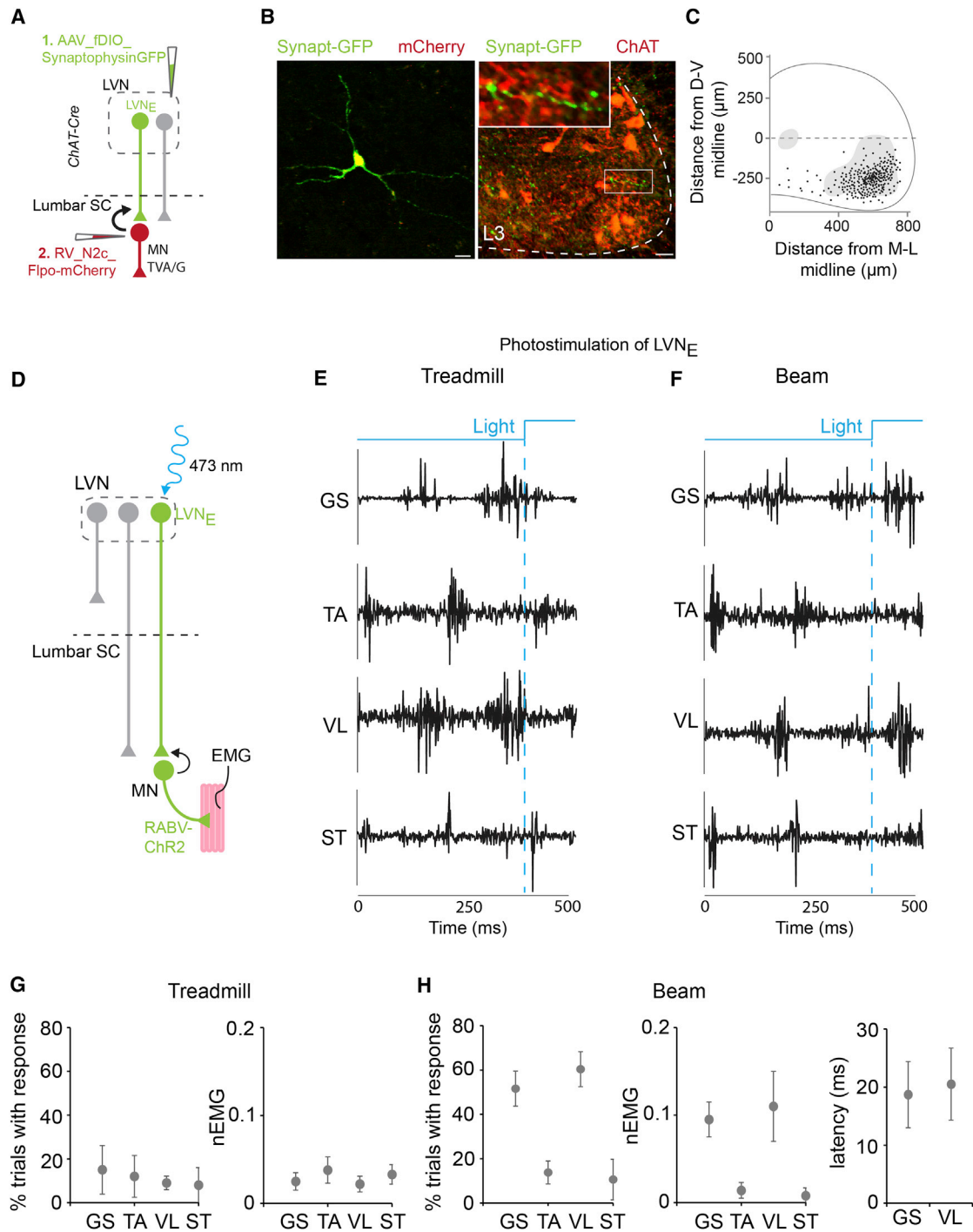


**Figure 4. Selective Terminal Projections and Stimulation of LVN<sub>E</sub> Neurons**

(A) Strategy for selective labeling of LVN<sub>E</sub> synaptic terminals.

(B) Example LVN<sub>E</sub> neuron in the LVN (left) and terminals (right) in the spinal cord. Scale bars, 30 μm.

(C) Contour density plot of LVN<sub>E</sub> synaptic terminals in the lumbar spinal cord. Gray shaded areas represent cholinergic neurons.

(D) Strategy for selective photoactivation of LVN<sub>E</sub> neurons.

(E) Illustrative EMG signals in GS, TA, ST, and VL muscles during treadmill walking with ChR2 photostimulation.

(F) Illustrative EMG signals in GS, TA, ST, and VL muscles during balance-beam walking with ChR photostimulation.

(legend continued on next page)

(Figure S4). Analysis of the pattern of LVN inputs at mid-lumbar levels revealed that LVN synapses were found on the distal dendrites of extensor motor neurons, >100  $\mu\text{m}$  from the neuronal cell body, with few, if any, synaptic contacts found on motor neuron somata (Figure S4). The selective monosynaptic innervation of extensor motor neurons is consistent with physiological observations in cat (Grillner et al., 1970; Wilson and Yoshida, 1969) and recent anatomical observations in mouse (Basaldella et al., 2015).

To probe whether single LVN neurons innervate multiple extensor pools, we used a two-color rabies virus retrograde-tracing strategy (Figure S4). RABV- $\Delta\text{G}$ -tdTomato was injected into the VL muscle, and RABV- $\Delta\text{G}$ -GFP was injected into the GS muscle in a single animal. Under these conditions, between 5% and 15% of rabies-infected LVN neurons expressed both GFP and tdTomato. This likely represents an underestimate of co-innervation due to the difficulty of infecting single neurons with two different rabies virions and is consistent with the idea that some LVN neurons exert coordinate control of extensor motor pools innervating different joints. This finding lends support to a view in which descending systems involved in responses to balance perturbation recruit synergist muscle groups as an ensemble rather than individually (Ting and McKay, 2007).

### Restricted Somatic Location and Terminal Distribution of LVN<sub>E</sub> Neurons Is Indicative of a Distinct Subclass

We next asked whether LVN neurons that activate extensor motor neuron pools represent a distinct subclass, assessed by somatic segregation and intraspinal terminal distribution.

To examine the somatic position of all lumbar-projecting LVN neurons, we injected the retrograde tracer FG into the L3 spinal cord. FG-labeled LVN neurons were dispersed throughout the rostro-caudal and dorso-ventral aspects of the LVN (Figure 3C), consistent with prior studies in mice (Liang et al., 2014). By quantifying the position of LVN<sub>E</sub> neurons after rabies tracing from GS and VL extensor pools, we observed that these sets of neurons were restricted to an intermediate region along the dorso-ventral axis (Figure 3D), consistent with the idea that LVN<sub>E</sub> neurons constitute a distinct subpopulation.

To explore this issue further, we examined whether LVN<sub>E</sub> neurons project to restricted domains in the ventral spinal cord. We first mapped the terminal distribution of the entire LVN population by injecting a recombinant AAV encoding GFP-tagged synaptophysin into the LVN and tracing the distribution of marked terminals within the ventral spinal cord. We found that the entire population of LVN neurons gives rise to a diffuse terminal arbor that extends broadly within the ventral lumbar spinal cord (Figure S5; see also Liang et al., 2014, and Basaldella et al., 2015, showing similar distributions). Additional synaptic terminal domains were detected in the medullary reticular nuclei (MRNs) and PRNs of the brainstem (Figure S5).

To map selectively the distribution of synaptic terminals of LVN<sub>E</sub> neurons, we developed a combinatorial rabies-AAV

approach that permits expression of GFP-tagged synaptophysin selectively in LVN<sub>E</sub> neurons. Separate AAV constructs encoding a cre-dependent version of rabies CVS-N2c glycoprotein (RABV-G; Reardon et al., 2016) and the avian receptor TVA were injected into the GS muscle of postnatal day (P)1–P4 *ChAT::Cre* animals, thus directing expression of RABV-G and TVA within GS motor neurons. After mice had reached adulthood, an AAV construct encoding a flip-recombinase-dependent synaptophysin-GFP was injected into the LVN. Three days after LVN AAV injection, an EnvA-pseudotyped CVS-N2c rabies virus encoding Flpo (Reardon et al., 2016) was injected into the lumbar spinal cord. Under these conditions, rabies virus selectively infects GS muscle-innervating motor neurons and is transferred retrogradely into premotor LVN neurons (Figure 4A). Within the vestibular nucleus, LVN<sub>E</sub> neurons alone are predicted to be infected by rabies virus, so that Flpo expression mediates recombination and expression of synaptophysin-GFP selectively in LVN<sub>E</sub> terminals in the spinal cord (Figure 4A).

We observed the labeling of 2–3 LVN<sub>E</sub> neurons in each mouse ( $n = 6$  animals) and between 50 and 100 synaptophysin-positive terminals per animal (Figure 4B). In the lumbar spinal cord, the vast majority (~80%) of LVN<sub>E</sub> synaptic terminals were localized within lamina IX of the ventral horn and in a small proportion of laminae VII (Figures 4B and 4C), a termination pattern much more restricted than that observed when synaptophysin-GFP was expressed in all lumbar-projecting LVN neurons (Figure S5). Thus, LVN neurons that innervate extensor motor neurons exhibit a highly restricted profile of arborization and termination. Moreover, we did not observe GFP<sup>+</sup> puncta in the PRN or medullary reticular nucleus (MRN) (data not shown), indicating that LVN<sub>E</sub> neurons lack brainstem collaterals.

### Selective Activation of LVN<sub>E</sub> Neurons Directs Extensor, but Not Flexor, Muscle Activity

The anatomical specificity of extensor motor neuron innervation by LVN neurons prompted us to examine whether selective activation of LVN<sub>E</sub> neurons is sufficient to trigger extensor muscle activity.

We used a RABV-based approach to direct Channelrhodopsin-2 (ChR2) expression selectively to LVN<sub>E</sub> neurons (Figure 4D). In the spinal cord of adult *ChAT::Cre* mice, two cre-dependent AAVs, one encoding CVS-N2c strain glycoprotein coupled to a histone GFP reporter and one encoding the TVA receptor, were injected selectively into the lateral ventral horn at lumbar (L3–L4) levels. In each animal, post hoc histology was used to verify that rabies glycoprotein was not expressed by pericentral cholinergic V0c neurons (Zagoraïou et al., 2009). After a further 2 weeks, to permit TVA and rabies glycoprotein expression, EnvA-pseudotyped CVS-N2c rabies virus encoding ChR2 (Reardon et al., 2016) was injected into the same site. Such injections resulted in the labeling of  $32 \pm 5$  LVN neurons per animal ( $n = 3$  animals). Ten days after rabies injection, an implanted optical fiber was used to activate LVN neurons by exposure to

(G) Number of trials that generated an EMG response (left) and normalized EMG values during treadmill walking with photostimulation ( $n = 5$  animals).

(H) Number of trials that generated an EMG response (left) and normalized EMG values and latency during balance-beam walking with photostimulation ( $n = 5$  animals).

SC, spinal cord; MN, motor neuron; G, glycoprotein. Data presented as mean  $\pm$  SEM.

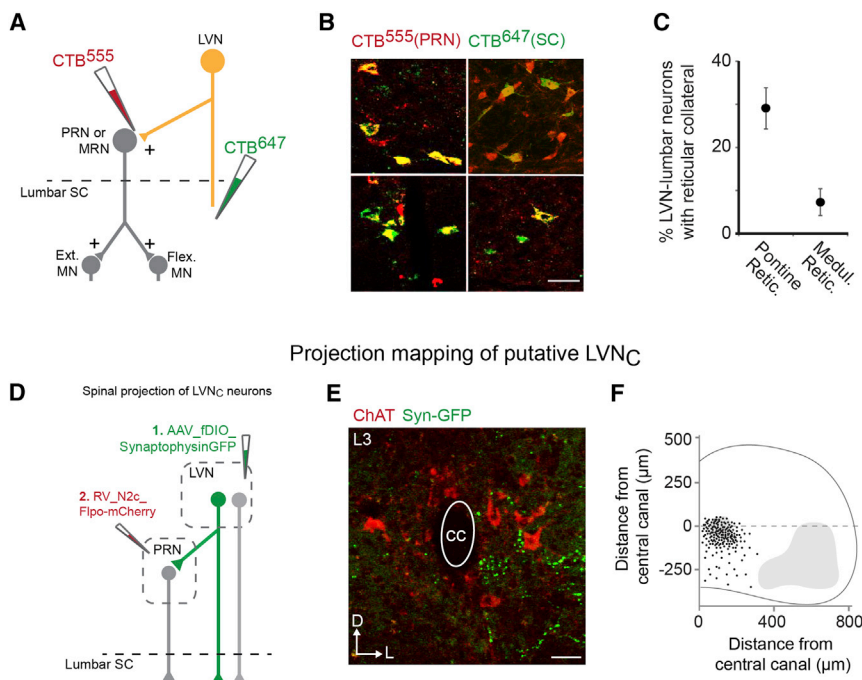


**Figure 5. Anatomical Characterization of LVN<sub>C</sub> Neurons**

(A) Strategy to identify whether lumbar LVN neurons send collaterals to reticular regions of the brainstem.

(B) Double-labeled neurons in the LVN after injection of CTB in the spinal cord and PRN.

(C) Quantitation of neurons in the LVN that send collaterals to the PRN or MRN as well as projecting to the lumbar spinal cord.

(D) Strategy to map the synaptic terminals of LVN neurons that project to the PRN (putative LVN<sub>C</sub> neurons).

(E) Terminals of LVN<sub>C</sub> neurons close to the central canal in the lumbar spinal cord.

(F) Contour density plot of LVN<sub>C</sub> neuron terminals in the lumbar spinal cord. Scale bars in (B) and (E), 30  $\mu$ m. cc, central canal; L3, lumbar level 3.

Data presented as mean  $\pm$  SEM.

473-nm laser light, while we monitored hindlimb muscle activity with EMG recordings (Figures 4D–4F).

Photo-stimulation of LVN<sub>E</sub> neurons was examined in two behavioral conditions: while mice were walking at a slow speed (0.1 m/s) on a treadmill and while traversing the balance beam. The speed of the treadmill was chosen roughly to match the speed at which the animals traversed the balance beam. We found that, during treadmill walking, pulsed activation of 473-nm laser light did not alter ongoing EMG activity with the normal extensor/flexor alternation phases of the step cycle (Figures 4E and 4G).

However, when assayed during balance beam walking, optogenetic activation of LVN<sub>E</sub> neurons led to clear EMG activity in 40%–60% of GS muscle trials and in 50%–70% of VL muscle trials during periods when flexor muscles should normally have been active (Figures 4F and 4H;  $p = 0.041$  for GS treadmill versus beam;  $p = 0.038$  for VL treadmill versus beam), whereas no activation of flexor muscles coincident with laser activation was observed (Figures 4F and 4H). The amplitude of the EMG signal in extensor responses was about one third of that seen after balance beam perturbation, likely due to the relatively small number of neurons infected with rabies-ChR2. The latency of EMG activation ranged from 12 to 25 ms after laser activation, a duration slightly longer than that seen for sensory-induced responses, which likely reflects the time required for ChR2 to activate LVN neurons. Thus, activation of LVN<sub>E</sub> neurons imposes extensor exclusivity in muscle activation.

### Lumbar Targeted LVN<sub>C</sub> Neurons Project Axons to the PRN

We next turned to the circuitry of antagonist muscle co-activation. Several lines of evidence have implicated the reticulo-spi-

nal pathways in both muscle co-activation and postural control. First, stimulation of the medial longitudinal fasciculus generates excitatory postsynaptic potentials (EPSPs) in both extensor and flexor lumbar motor neurons (Grillner and Lund, 1968; Peterson, 1979). The PRN and MRN represent the origin of a majority of reticulo-spinal fibers (Tohyama et al., 1979), and in mouse, both receive projections from the LVN (Figure S5). Second, the firing features of certain reticulospinal neuron classes correlate with postural correction after perturbation (Deliagina et al., 2014). Third, several brainstem reticular regions, including the PRN and MRN, exhibit rapid responses to vestibular stimulation (Mori et al., 2001; Wilkinson et al., 2004).

We examined first the involvement of the MRN and PRN brainstem nuclei for a possible role in LVN-generated co-activation. Dual-color retrograde labeling was performed to trace the brainstem collaterals of lumbar-projecting LVN neurons. A cholera toxin beta subunit (CTB) conjugated with Alexa Fluor 647 was injected into the lumbar spinal cord to label lumbar-projecting LVN neurons. In addition, CTB conjugated to Alexa Fluor 555 was injected separately into either the PRN or the MRN so that double-labeled neurons represent LVN neurons with projections both to lumbar spinal cord and one of these brainstem nuclei (Figure 5A). This analysis revealed that  $30 \pm 5\%$  of lumbar-projecting LVN neurons send axon collateral branches to the PRN, whereas only  $8 \pm 2.5\%$  of lumbar-projecting LVN neurons send collaterals to the MRN (Figures 5B and 5C). We further examined this LVN-PRN pathway by performing retrograde monosynaptic rabies tracing from L3 and L4 motor neurons to visualize premotor neurons in the PRN. In the same animals, we injected AAV-synaptophysin-GFP into the LVN to visualize LVN neuron synapses (Figure S6). In the PRN, we found numerous synaptic terminals closely apposed to PRN premotor somata (Figure S6). This finding indicates that the LVN may utilize a disynaptic pathway via the PRN to lumbar motor neurons to influence postural control.

Photostimulation of LVN<sub>C</sub>

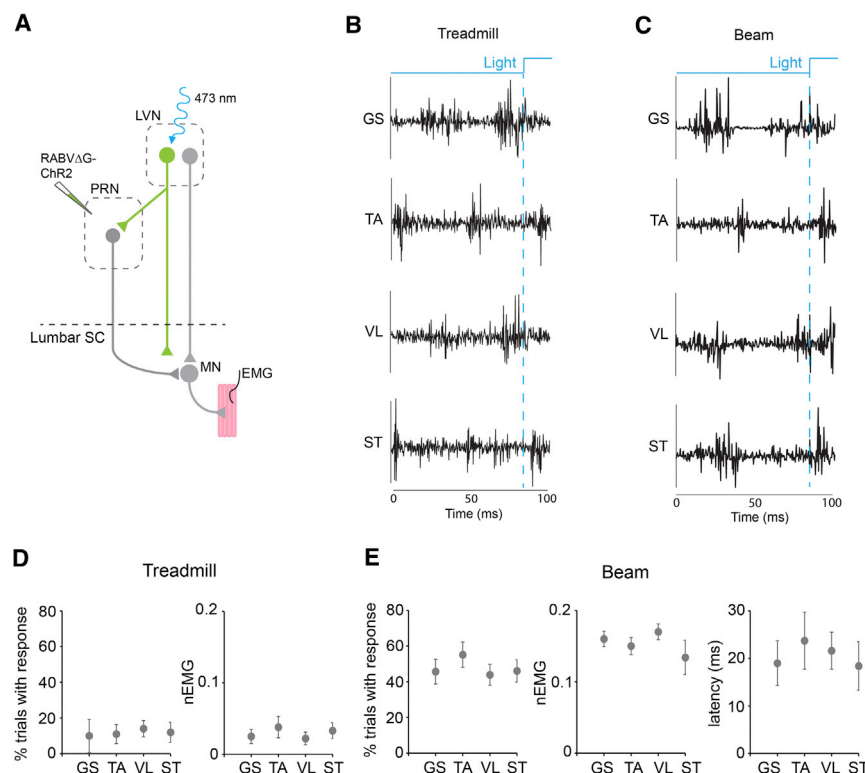


**Figure 6. Muscle Co-activation after Selective Photostimulation of LVN<sub>C</sub> Neurons**

(A) Strategy for selective expression of ChR in LVN<sub>C</sub> neurons.

(B) Illustrative EMG recordings in the GS, TA, VL, and ST muscles with photostimulation of LVN<sub>C</sub> neurons during treadmill walking.

(C) Illustrative EMG recordings in the GS, TA, VL, and ST muscles with photostimulation of LVN<sub>C</sub> neurons during balance beam walking.

(D) Number of trials with EMG responses (left) and normalized EMG signals (right) during treadmill walking (n = 3 animals).

(E) Number of trials with EMG responses (left) normalized EMG (middle) and latency of response (right) from photostimulation during balance beam walking (n = 3 animals).

Data presented as mean ± SEM.

encoding hChR2-eYFP (Reardon et al., 2016) into the PRN in order to infect the terminals of LVN neurons (Figure 6A). This method labeled  $52 \pm 10$  LVN neurons (n = 6 animals). We then selectively activated these LVN-PRN neurons using 473-nm wavelength illumination through an implanted fiber optic cannula.

LVN<sub>C</sub> photoactivation was carried out while animals walked at a slow speed (0.1 m/s) on a treadmill or freely traversed the balance beam.

During treadmill walking, we did not observe photo-stimulus-induced EMG activation (Figures 6B and 6D). Nevertheless, in  $46.7 \pm 7.5\%$  of trials during beam walking (mean for all muscles), we observed an interruption of the ongoing step cycle and co-activation of GS and VL extensor as well as TA and ST flexor muscles, with a delay of  $21.1 \pm 3.1$  ms after the onset of photo-stimulation (Figures 6C and 6E). The amplitude of co-activation was about one-quarter of that seen during beam perturbations (nEMG values in Figure 1, compared with Figure 6E), potentially due to the small number of neurons expressing ChR2. Control animals who received an injection of RABV-N2c-ΔG-GFP into the PRN and fiber optic implantation into the LVN did not exhibit light-related EMG activity when walking on the balance beam (Figure S6). We conclude that stimulation of LVN neurons that project to the PRN elicits co-activation of hindlimb extensor and flexor muscles, supporting their designation as LVN<sub>C</sub> neurons.

**The PRN Promotes Balance Perturbation-Initiated Co-activation**

To evaluate the contribution of spinally projecting PRN neurons to co-activation, we examined their impact on balance correction. Lumbar-projecting PRN neurons were targeted using an intersectional lesion strategy. An AAV encoding a GFP-tagged DTR was injected into the PRN, followed 3 weeks later by local injection of DT into the L3 spinal cord (Figure 7A; Figure S6). We reasoned that, if PRN neurons are involved in the generation

To examine whether LVN<sub>C</sub> neurons represent a distinct LVN subtype, we compared their terminal distribution in the spinal cord with that of the LVN<sub>E</sub> neuronal population. To achieve this, synaptophysin-GFP was expressed in LVN<sub>C</sub> neurons using an intersectional AAV-rabies virus strategy. A Flp-dependent AAV encoding synaptophysin-GFP was injected into the LVN, and after a further 7 days, glycoprotein-coated rabies virus encoding Flpo-mCherry was injected into the PRN. Rabies virus-mediated Flpo expression in LVN neurons will direct synaptophysin-GFP expression selectively within this set of LVN<sub>C</sub> neurons (Figure 5D).

Analysis of the position of GFP<sup>+</sup> puncta in the lumbar spinal cord indicates that ~75% of LVN-PRN terminals were restricted to a region just lateral and ventral to the central canal (Figures 5E and 5F). Most LVN<sub>C</sub> boutons were found near V0c neurons and medially positioned V2a neurons, and all were located in the medial spinal cord within 350 μm of the central canal, but strikingly, projections and boutons were not observed within the motor neuron cell body region (Figure 5F). Thus, the positioning of LVN<sub>C</sub> axons in spinal cord differs from that of LVN<sub>E</sub> neurons. These data indicate that LVN<sub>C</sub> neurons with collaterals in the PRN represent an anatomically distinct subset of spinally projecting LVN neurons.

**Activation of LVN<sub>C</sub> Neurons Elicits Co-activation of Extensor and Flexor Muscles**

We examined whether activation of PRN-projecting LVN neurons can generate hindlimb antagonist muscle co-activation using a rabies virus strategy. We injected rabies virus CVS-N2c

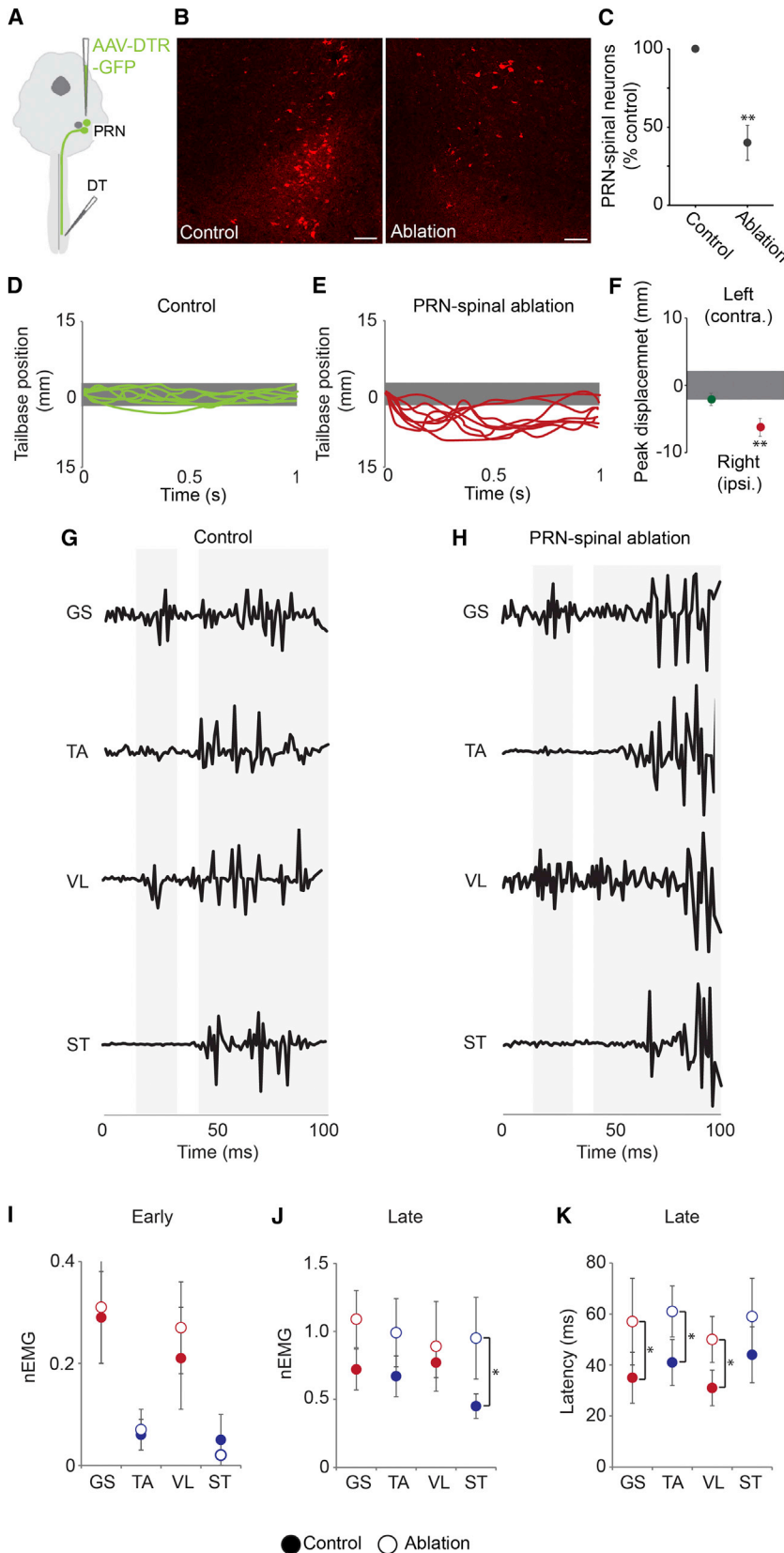


**Figure 7. Balance Impairment after Ablation of Spinally Projecting PRN Neurons**

(A) Strategy to selectively ablate spinally projecting PRN neurons.

(B) PRN neurons retrogradely labeled from the spinal cord, with and without ablation. Scale bars, 150  $\mu$ m.

(C) Quantitation of ablation of spinally projecting PRN neurons.

(D) Tail-base position of control animals during balance beam perturbation.

(E) Tail-base position of animals during balance beam perturbation after ablation of spinally projecting PRN neurons.

(F) Illustrative EMG signals in the GS, TA, VL, and ST muscles in control animals after balance beam perturbation at time 0.

(G) Illustrative EMG signals in the GS, TA, VL, and ST muscles in PRN spinal ablated animals after balance beam perturbation.

(H) Quantitation of normalized EMG response in the early phase of control and ablated animals (n = 5 animals).

(I) Quantitation of normalized EMG response in the early phase of control and ablated animals (n = 5 animals).

(J) Quantitation of normalized EMG response in the late phase of control and ablated animals (n = 5 animals).

(K) Onset latency for the late-phase EMG response in control and ablated animals (n = 5 animals).

Data are shown as mean  $\pm$  SEM in (C) and mean  $\pm$  SD in (H)–(J). \*p < 0.05; \*\*p < 0.01.

of co-activation, their ablation might be expected to result in a delay or absence of muscle co-activation.

The effectiveness of the ablation was assessed by FG injection into the L3 spinal cord to retrogradely label residual lumbar spinal-projecting PRN neurons. This revealed a  $56 \pm 7\%$  reduction in the number of lumbar spinal PRN neurons compared to the contralateral side (non-AAV injected;  $n = 6$  animals;  $p = 0.011$ ) (Figures 7A–7C). Mice with DT-induced lumbar-projecting PRN neuron deletions were impaired in their ability to maintain center of mass following balance beam displacement (Figures 7D–7F). In PRN-ablated mice, the mean displacement of the tail-base position increased to  $4.1 \pm 1.1$  mm from the bounds of the beam, compared with control mice whose tail-base position was kept above the beam (Figure 7F).

We next performed EMG recordings from the GS, TA, VL, and ST muscles. The amplitude of the early extensor selective response for GS and VL muscles was similar to that for control animals (Figures 7G–7I), and there was no change in onset latency (GS latency:  $21.5 \pm 4.2$  ms for control versus  $19.9 \pm 3.7$  ms for ablation; VL latency:  $20.6 \pm 3.7$  ms for control versus  $21.9 \pm 4.1$  ms for ablation). However, analysis of the late response in control animals revealed an overall increase in latency from perturbation onset from  $35 \pm 4$  ms to  $58 \pm 5$  ms in PRN-ablated mice ( $n = 6$  animals;  $p = 0.022$  for all muscles; Figure 7K). We also saw an overall increase in normalized EMG amplitude during the 50- to 100-ms epoch from perturbation onset, which reached statistical significance in the ST muscle ( $p = 0.041$ ) (Figure 7J). In addition, the EMG burst response continued for an additional  $51 \pm 14$  ms in PRN-ablated animals. Thus, disruption of pontine reticulo-spinal neurons results in a significant delay in the generation of balance-perturbation-induced co-activation (Figure 7K).

We note that  $LVN_C$  neurons project to the ventral spinal cord as well as the PRN and, thus, could potentially achieve antagonist co-activation via facilitation of motor neuron output through recruitment of spinal excitatory interneurons. We tested whether the major class of ventral excitatory premotor interneurons, glutamatergic V2a interneurons, many of which are located in the termination zone of  $LVN_C$  projections (Zhong et al., 2010), contribute to the output of  $LVN_C$  neurons. In *Chx10::Cre* mice, we ablated V2a neurons from L2–L6 spinal cord by lumbar spinal injection of a cre-dependent AAV-encoding DTR (Crone et al., 2009). After a further 14 days, DT was administered intraperitoneally, resulting in a reduction to  $57.4 \pm 6.2\%$  of lumbar V2a interneurons compared to control.

Prior to DT injection, control animals ( $n = 4$ ) were induced to walk on a treadmill with alternating gaits until speeds of  $>0.7$  m/s were obtained (Figure S7). In contrast, DT-treated animals exhibited a marked hopping gait on the treadmill at speeds greater than 0.4 m/s, consistent with previous analyses (Crone et al., 2009). However, after DT injection, EMG responses in both the early extension and late co-activation phases were comparable to those of controls (Figure S7). We conclude that a full complement of V2a interneurons is not required for extensor-flexor co-activation. It is not possible to exclude that non-V2a excitatory interneuron pathways serve such a role, however. Nevertheless, our studies indicate that monosynaptic input from PRN reticulo-spinal neurons to both flexor and

extensor motor neurons is likely to serve a crucial role in the generation of muscle co-activation (Fukushima et al., 1979; Wilson and Yoshida, 1968).

## DISCUSSION

When balance is perturbed, ongoing motor programs are switched to contextually appropriate muscle activation patterns that maintain body posture. We show here that the LVN can respond to a balance perturbation by generating a motor program of muscle extension, followed some 30 ms later by co-activation of antagonist muscles in the hindlimb. This program appears to engage anatomically and functionally distinct classes of LVN neuron that work together to generate this reflex-triggered instance of adaptive motor behavior.

### Anatomical and Functional Heterogeneity within the LVN

Physiological studies of LVN output have focused largely on its role in activating extensor muscles (Grillner and Hongo, 1972; Orlovsky, 1972), but a functional description of the LVN's role in postural control is lacking. Studies have hinted at LVN cell-type diversity in terms of neuronal size, physiological properties, conduction velocity, and spinal projection (Shinoda et al., 1988, 1992; Pompeiano, 1991; Boyle et al., 2004), raising the possibility that multiple LVN cell types exist and coordinate different aspects of balance correction.

In mice, we find that balance perturbation during beam walking results in three temporally separated phases of hindlimb EMG response. An initial phase of exclusive extensor motor neuron and muscle activity likely serves to extend the hindpaws and return or maintain their position on the balance beam. A second phase is characterized by little extensor or flexor muscle activation. This second phase could potentially reflect the attenuation of reciprocal inhibitory interneuron activity, effectively “priming” motor circuits during the transition to co-activation by removing a tonic inhibitory drive to flexor motor neurons (Nielsen and Kagamihara, 1992; Nielsen and Pierrot-Deseilligny, 1996). A functional coupling between the vestibular system and Renshaw interneurons has been documented, although the circuit basis of such interactions remains unclear (Pompeiano, 1988). Nevertheless, we have observed synaptic inputs directly from the LVN to  $\sim 40\%$  of lumbar spinal Renshaw neurons (A.J.M. and T.M.J., unpublished data), implying direct LVN control of the Renshaw output to reciprocal inhibitory interneurons. As we did not observe input from  $LVN_E$  or  $LVN_C$  to Renshaw neurons, this may indicate a third discrete population of LVN neurons. The lack of selective markers for Renshaw neurons, however, means that we have been unable to evaluate this LVN population. The third phase of antagonist muscle co-activation appears to provide stiffness and resistive strength at the hindlimb joints to accommodate reactive ground forces.

The temporal sequence of recruitment of LVN neurons cannot easily be explained by downstream synaptic delays and is likely to reflect temporal differences in timing of inputs to LVN populations, presumably from different neuronal sources. We note that PRN ablation did not result in a complete loss of co-activation but, rather, caused this phase to be delayed. Pontine

reticulo-spinal projections may represent an initial pathway recruited by the LVN to generate muscle co-activation. Disruption of this pathway, and a consequent lack of postural correction, could result in continuing sensory drive to the LVN, generating longer and larger co-activation signals.

Our studies, therefore, point to the presence of two distinct neuronal classes within the LVN. The cell bodies of LVN<sub>E</sub> neurons are restricted medially within the LVN, their spinal axonal arbors are confined to the motor neuron domain, and they directly innervate extensor motor neurons. In contrast, LVN<sub>C</sub> axon terminals are restricted to a region adjacent to the central canal, and unlike LVN<sub>E</sub> neurons, they also send axonal collaterals to the PRN. Optogenetic activation of the LVN<sub>E</sub> or LVN<sub>C</sub> populations resulted in activation of either extensors alone (LVN<sub>E</sub>) or extensors and flexors jointly (LVN<sub>C</sub>). A current lack of genetic markers for these populations meant that we were unable to perform selective ablation of these two populations and examine the effect on early- and late-phase muscle activations.

The termination zone of LVN<sub>C</sub> neurons coincides both with medial V2a and cholinergic V0<sub>C</sub> interneurons (Zagoraïou et al., 2009), but inactivation of a majority of V2a interneurons failed to impact LVN<sub>C</sub> mediated co-activation. Cholinergic V0<sub>C</sub> neurons have been implicated in task-specific gain control in spinal motor systems (Zagoraïou et al., 2009). If LVN<sub>C</sub> neurons do form direct connections with V0<sub>C</sub> interneurons, it is possible that activation of V0<sub>C</sub> neurons, via post-synaptic muscarinic receptors, will sensitize motor neurons (Witts et al., 2014) and contribute to muscle co-activation. Motor responses to balance perturbations are highly dependent on context (Jacobs and Horak, 2007), and it therefore seems likely that further cell types exist within the LVN, activating different muscle synergies according to biomechanical constraint.

#### **Temporal Segregation of LVN Output**

The broad temporal segregation of EMG response and, by implication, the differential recruitment of LVN<sub>E</sub> and LVN<sub>C</sub> neurons cannot easily be explained by synaptic delays in the output of these neurons. The polysynaptic nature of the LVN-PRN pathway for co-activation would likely add only 2–3 ms for each synapse in output pathway, compared to the monosynaptic LVN<sub>E</sub> pathway that directly activates extensor motor neurons. Different axonal diameters and, therefore, conduction velocities of LVN and PRN neurons may underlie the temporal difference between extension and coactivation (Pompeiano, 1991); however, even with slower axonal transmission and a polysynaptic pathway, it seems unlikely that this delay would reach 30 ms. Thus, a combination of circuit and axonal structure, as well as the inputs to these two neuronal classes, could contribute to the timing of activation.

The LVN receives input from a variety of sensory and other sources, notably from primary vestibular afferents, cerebellar Purkinje cells, brainstem regions, and primary motor cortex, as well as somatosensory input concerning limb position and direction of movement (Pompeiano, 1972; Sarkisian, 2000; McCall et al., 2016). Studies in humans have indicated that the initial response to vestibular stimulation and the generation of limb extension relies on input from the otolith organs and is the result of an unexpected acceleration (Cathers et al., 2005). In our

studies, initial horizontal beam acceleration is likely to be sensed by the utricle, and studies in cats have demonstrated direct utricular sensory input to vestibulospinal neurons (Kushiro et al., 2000). If this circuitry is pertinent, LVN<sub>E</sub> neurons would be expected to receive direct input from otolith vestibular afferents. Recently, subpopulations of vestibular nuclei neurons in the cat have been shown to alter their firing in response to extension, flexion, or unidirectional movements of the hindlimb (McCall et al., 2016). Given the importance of somatosensory information for postural control (Karayannidou et al., 2009; Hsu et al., 2017), it seems likely that the LVN serves to integrate multiple modalities of sensory information concerning body and limb position and movement, with activation of a select set of these inputs recruiting a subpopulation of LVN neurons to appropriately modify spinal motor programs.

In contrast to extensor responses, hindlimb co-activation has not previously been reported in response to LVN stimulation (Deliagina et al., 2014). This may reflect the use of decortical or decerebrate animals in previous studies of LVN function. Muscle co-activation can be triggered by input from cortical or cerebellar motor circuits (Fetz and Cheney, 1987; Smith, 1981; Humphrey and Reed, 1983). Moreover, stimulation of either extensor or flexor motor cortical regions can enhance LVN neuron firing (Licata et al., 1990). Vestibular sensory information ascends to several cortical regions, notably, the primary motor cortex (Rancz et al., 2015), where it can be integrated with proprioceptive and cutaneous inputs and with other sensory modalities involved in generating contextually relevant responses to balance beam perturbation, providing a mechanism for complex, context-specific, postural reflexes (Jacobs and Horak, 2007). Thus, late-phase co-activation could represent a cortical loop that integrates multiple sensory modalities and controls the late activation of LVN<sub>C</sub> neurons. In this way, the motor cortex could provide a context-specific permissive signal for LVN<sub>C</sub> neurons to drive hindlimb co-activation.

#### **Context Specificity of Vestibulospinal Control**

One striking feature of our functional analysis is that ChR-mediated stimulation of LVN<sub>E</sub> or LVN<sub>C</sub> populations results in a task dependency of EMG activation. Activation of LVN<sub>E</sub> or LVN<sub>C</sub> neurons generated an EMG response only when animals traversed a balance beam and not during treadmill walking. One potential mechanism involves differences in proprioceptive signaling from the hindlimb under conditions of treadmill or beam walking. A narrower stance would require increased muscle tension to support the body on the beam, likely increasing proprioceptive sensory input to motor neurons and bringing them closer to an activation threshold, so that they become responsive to vestibulospinal input.

Additionally, it is conceivable that, during treadmill walking, the spinal circuitry dominates and the drive from locomotor interneurons to motor neurons cannot be overcome with LVN<sub>E</sub> or LVN<sub>C</sub> stimulation, whereas during a balancing task, descending inputs are favored. It is possible, therefore, that stimulation of a greater number of LVN neurons, or a broader range of LVN classes, would influence treadmill locomotion. However, these results do hint at an external mechanism increasing the gain of relevant LVN vestibulospinal output systems on the balance beam.

## EXPERIMENTAL PROCEDURES

Further information is available in the [Supplemental Experimental Procedures](#).

### Experimental Model and Subject Details

All procedures were performed on mice. Procedures performed in this study were conducted according to U.S. NIH guidelines for animal research and were approved by the Institutional Animal Care and Use Committee of Columbia University Medical Center, protocol number AAAG8461, or under UK Home Office license according to the United Kingdom Animals (Scientific Procedures) Act 1986.

Chat-IRES-Cre (Jackson Laboratory, stock number 006410; Rossi et al., 2011) mice were used to drive cre expression in motor neurons; and RGT mice, for cre-conditional expression of rabies B19 glycoprotein and the TVA (Takato et al., 2013), were used to express rabies glycoprotein for monosynaptic tracing using the SAD-B19 rabies virus.

For behavioral studies, both male and female animals were used. Unless otherwise stated, animals were always between 8 and 12 weeks of age. A total of 25 animals were used for behavioral studies comprising 19 wild-type C57/Bl6 animals (LVN ablation studies,  $n = 8$ ; PRN spinal ablation studies,  $n = 5$ ; LVN<sub>C</sub> optogenetic stimulation and control,  $n = 6$ ), 5 ChAT::Cre animals (LVN<sub>E</sub> optogenetic stimulation), and 4 Chx10::Cre animals (V2a ablation). Animals were group housed until implantation of EMG electrodes, when they were individually housed to prevent damage to hindlimb surgical incisions. For anatomical studies, a total of 25 animals were used, comprising 6 RGT, Chat::Cre, 6 ChAT::Cre, and 13 wild-type C57/Bl6.

### Statistical Analysis

Results are expressed as the mean  $\pm$  SD, unless otherwise stated. Statistical analysis was carried out in Spike2, R, or Microsoft Excel. Normality of the distribution was confirmed using a Shapiro-Wilks test. For evaluation of EMG data, one- or two-way ANOVAs were used on the rectified EMG signal. Unpaired Student's *t* tests were used for comparison of normalized EMG (nEMG) signals and for quantification of ablation efficiency. Unpaired Student's *t* tests were used for all other analyses.  $p < 0.05$  was considered significant.

## SUPPLEMENTAL INFORMATION

Supplemental Information includes Supplemental Experimental Procedures and seven figures and can be found with this article online at <https://doi.org/10.1016/j.celrep.2018.01.009>.

## ACKNOWLEDGMENTS

We are grateful to Staceyann Doobar, Monica Mendelsohn, Carolyn Diaz, Alexandra Kauffman, and Emily Reader-Harris for technical assistance with experiments and Susan Morton for advice on antibodies. Thomas Reardon and Timothy Machado contributed useful discussions, and Ira Schieren provided computational advice and imaging expertise. Tatiana Deliagina provided insightful comments on vestibular control systems, and we benefitted from numerous discussions of vestibular function with Jens Bo Nielsen. Richard Axel, Nikos Balaskas, Sara Fenstermacher, Andrew Miri, and Anders Nelson provided helpful comments on the manuscript. pAAV-fDIO-eYFP was a gift from Karl Deisseroth (Addgene plasmid 55641). A.J.M. is supported by the Gatsby Charitable Foundation and the Wellcome Trust. T.M.J. was supported by NIH grant NS0332245, the Mathers Foundation, and Project ALS and is a HHMI Investigator.

## AUTHOR CONTRIBUTIONS

A.J.M. and T.M.J. conceived the project. A.J.M., T.M.J., T.B., and T.A. designed the experiments. A.J.M., T.B., and K.C. performed experiments and analyzed the data, with input from T.M.J. and T.A. A.J.M. and T.M.J. wrote the manuscript, with input from all other authors.

## DECLARATION OF INTERESTS

The authors declare no competing interests.

Received: March 10, 2017

Revised: November 29, 2017

Accepted: January 3, 2018

Published: January 30, 2018

## REFERENCES

- Akay, T., Tourtellotte, W.G., Arber, S., and Jessell, T.M. (2014). Degradation of mouse locomotor pattern in the absence of proprioceptive sensory feedback. *Proc. Natl. Acad. Sci. USA* *111*, 16877–16882.
- Allum, J.H.J., and Honegger, F. (2013). Relation between head impulse tests, rotating chair tests, and stance and gait posturography after an acute unilateral peripheral vestibular deficit. *Otol. Neurotol.* *34*, 980–989.
- Basaldella, E., Takeoka, A., Sigrist, M., and Arber, S. (2015). Multisensory signaling shapes vestibulo-motor circuit specificity. *Cell* *163*, 301–312.
- Beloozerova, I.N., Zelenin, P.V., Popova, L.B., Orlovsky, G.N., Grillner, S., and Deliagina, T.G. (2003). Postural control in the rabbit maintaining balance on the tilting platform. *J. Neurophysiol.* *90*, 3783–3793.
- Boyle, R., Bush, G., and Ehsanian, R. (2004). Input/output properties of the lateral vestibular nucleus. *Arch. Ital. Biol.* *142*, 133–153.
- Canedo, A. (1997). Primary motor cortex influences on the descending and ascending systems. *Prog. Neurobiol.* *51*, 287–335.
- Cathers, I., Day, B.L., and Fitzpatrick, R.C. (2005). Otolith and canal reflexes in human standing. *J. Physiol.* *563*, 229–234.
- Chvatal, S.A., Macpherson, J.M., Torres-Oviedo, G., and Ting, L.H. (2013). Absence of postural muscle synergies for balance after spinal cord transection. *J. Neurophysiol.* *110*, 1301–1310.
- Crone, S.A., Zhong, G., Harris-Warrick, R., and Sharma, K. (2009). In mice lacking V2a interneurons, gait depends on speed of locomotion. *J. Neurosci.* *29*, 7098–7109.
- Deliagina, T.G., Beloozerova, I.N., Orlovsky, G.N., and Zelenin, P.V. (2014). Contribution of supraspinal systems to generation of automatic postural responses. *Front. Integr. Neurosci.* *8*, 76.
- Di Bonito, M., Boulland, J.-L., Krezel, W., Setti, E., Studer, M., and Glover, J.C. (2015). Loss of projections, functional compensation, and residual deficits in the mammalian vestibulospinal system of Hoxb1-deficient mice. *eNeuro* *2*, ENEURO.0096-15.2015.
- Fetz, E.E., and Cheney, P.D. (1987). Functional relations between primate motor cortex cells and muscles: fixed and flexible. *Ciba Found. Symp.* *132*, 98–117.
- Fukushima, K., Peterson, B.W., and Wilson, V.J. (1979). Vestibulospinal, reticulospinal and interstitiospinal pathways in the cat. *Prog. Brain Res.* *50*, 121–136.
- Goldberg, J.M., and Cullen, K.E. (2011). Vestibular control of the head: possible functions of the vestibulocollic reflex. *Exp. Brain Res.* *210*, 331–345.
- Grillner, S., and Hongo, T. (1972). Vestibulospinal effects on motoneurons and interneurons in the lumbosacral cord. *Prog. Brain Res.* *37*, 243–262.
- Grillner, S., and Lund, S. (1968). The origin of a descending pathway with monosynaptic action on flexor motoneurons. *Acta Physiol. Scand.* *74*, 274–284.
- Grillner, S., Hongo, T., and Lund, S. (1970). The vestibulospinal tract. Effects on alpha-motoneurons in the lumbosacral spinal cord in the cat. *Exp. Brain Res.* *10*, 94–120.
- Grillner, S., Hongo, T., and Lund, S. (1971). Convergent effects on alpha motoneurons from the vestibulospinal tract and a pathway descending in the medial longitudinal fasciculus. *Exp. Brain Res.* *12*, 457–479.
- Hardisty-Hughes, R.E., Parker, A., and Brown, S.D.M. (2010). A hearing and vestibular phenotyping pipeline to identify mouse mutants with hearing impairment. *Nat. Protoc.* *5*, 177–190.

- Honegger, F., Hillebrandt, I.M.A., van den Elzen, N.G.A., Tang, K.-S., and Al-lum, J.H.J. (2013). The effect of prosthetic feedback on the strategies and synergies used by vestibular loss subjects to control stance. *J. Neuroeng. Rehabil.* *10*, 115.
- Horak, F.B. (2009). Postural compensation for vestibular loss. *Ann. N Y Acad. Sci.* *1164*, 76–81.
- Hsu, L.J., Zelenin, P.V., Lyalka, V.F., Vemula, M.G., Orlovsky, G.N., and Deliagina, T.G. (2017). Neural mechanisms of single corrective steps evoked in the standing rabbit. *Neuroscience* *347*, 85–102.
- Humphrey, D.R., and Reed, D.J. (1983). Separate cortical systems for control of joint movement and joint stiffness: reciprocal activation and coactivation of antagonist muscles. *Adv. Neurol.* *39*, 347–372.
- Jacobs, J.V., and Horak, F.B. (2007). Cortical control of postural responses. *J. Neural Transm. (Vienna)* *114*, 1339–1348.
- Karayannidou, A., Beloozerova, I.N., Zelenin, P.V., Stout, E.E., Sirota, M.G., Orlovsky, G.N., and Deliagina, T.G. (2009). Activity of pyramidal tract neurons in the cat during standing and walking on an inclined plane. *J. Physiol.* *587*, 3795–3811.
- Kushiro, K., Zakir, M., Sato, H., Ono, S., Ogawa, Y., Meng, H., Zhang, X., and Uchino, Y. (2000). Saccular and utricular inputs to single vestibular neurons in cats. *Exp. Brain Res.* *131*, 406–415.
- Liang, H., Bácskai, T., Watson, C., and Paxinos, G. (2014). Projections from the lateral vestibular nucleus to the spinal cord in the mouse. *Brain Struct. Funct.* *219*, 805–815.
- Licata, F., Li Volsi, G., Maugeri, G., and Santangelo, F. (1990). Effects of motor cortex and single muscle stimulation on neurons of the lateral vestibular nucleus in the rat. *Neuroscience* *34*, 379–390.
- McCall, A.A., Miller, D.M., DeMayo, W.M., Bourdages, G.H., and Yates, B.J. (2016). Vestibular nucleus neurons respond to hindlimb movement in the conscious cat. *J. Neurophysiol.* *116*, 1785–1794.
- Mori, R.L., Bergsman, A.E., Holmes, M.J., and Yates, B.J. (2001). Role of the medial medullary reticular formation in relaying vestibular signals to the diaphragm and abdominal muscles. *Brain Res.* *902*, 82–91.
- Nielsen, J., and Kagamihara, Y. (1992). The regulation of disynaptic reciprocal Ia inhibition during co-contraction of antagonistic muscles in man. *J. Physiol.* *456*, 373–391.
- Nielsen, J., and Pierrot-Deseilligny, E. (1996). Evidence of facilitation of soleus-coupled Renshaw cells during voluntary co-contraction of antagonistic ankle muscles in man. *J. Physiol.* *493*, 603–611.
- Orlovsky, G.N. (1972). Activity of vestibulospinal neurons during locomotion. *Brain Res.* *46*, 85–98.
- Peterson, B.W. (1979). Reticulospinal projections to spinal motor nuclei. *Annu. Rev. Physiol.* *41*, 127–140.
- Pompeiano, O. (1972). Spinovestibular relations: anatomical and physiological aspects. *Prog. Brain Res.* *37*, 263–296.
- Pompeiano, O. (1988). The role of Renshaw cells in the dynamic control of posture during vestibulospinal reflexes. *Prog. Brain Res.* *76*, 83–95.
- Pompeiano, O. (1991). The role of different size vestibulospinal neurons in the static control of posture. *Arch. Ital. Biol.* *129*, 21–41.
- Rancz, E.A., Moya, J., Drawitsch, F., Brichta, A.M., Canals, S., and Margrie, T.W. (2015). Widespread vestibular activation of the rodent cortex. *J. Neurosci.* *35*, 5926–5934.
- Reardon, T.R., Murray, A.J., Turi, G.F., Wirblich, C., Croce, K.R., Schnell, M.J., Jessell, T.M., and Losonczy, A. (2016). Rabies virus CVS-N2c(ΔG) strain enhances retrograde synaptic transfer and neuronal viability. *Neuron* *89*, 711–724.
- Rossi, J., Balthasar, N., Olson, D., Scott, M., Berglund, E., Lee, C.E., Choi, M.J., Lauzon, D., Lowell, B.B., and Elmquist, J.K. (2011). Melanocortin-4 receptors expressed by cholinergic neurons regulate energy balance and glucose homeostasis. *Cell Metab.* *13*, 195–204.
- Sarkisian, V.H. (2000). Input-output relations of Deiters' lateral vestibulospinal neurons with different structures of the brain. *Arch. Ital. Biol.* *138*, 295–353.
- Shinoda, Y., Ohgaki, T., and Futami, T. (1986). The morphology of single lateral vestibulospinal tract axons in the lower cervical spinal cord of the cat. *J. Comp. Neurol.* *249*, 226–241.
- Shinoda, Y., Ohgaki, T., Sugiuchi, Y., and Futami, T. (1988). Structural basis for three-dimensional coding in the vestibulospinal reflex. Morphology of single vestibulospinal axons in the cervical cord. *Ann. N Y Acad. Sci.* *545*, 216–227.
- Shinoda, Y., Ohgaki, T., Sugiuchi, Y., Futami, T., and Kakei, S. (1992). Functional synergies of neck muscles innervated by single medial vestibulospinal axons. *Ann. N Y Acad. Sci.* *656*, 507–518.
- Smith, A.M. (1981). The coactivation of antagonist muscles. *Can. J. Physiol. Pharmacol.* *59*, 733–747.
- Takato, J., Nelson, A., Zhou, X., Bolton, M.M., Ehlers, M.D., Arenkiel, B.R., Mooney, R., and Wang, F. (2013). New modules are added to vibrissal premotor circuitry with the emergence of exploratory whisking. *Neuron* *77*, 346–360.
- Tang, P.F., Woollacott, M.H., and Chong, R.K. (1998). Control of reactive balance adjustments in perturbed human walking: roles of proximal and distal postural muscle activity. *Exp. Brain Res.* *119*, 141–152.
- Timmann, D., and Horak, F.B. (1998). Perturbed step initiation in cerebellar subjects. 1. Modifications of postural responses. *Exp. Brain Res.* *119*, 73–84.
- Ting, L.H., and McKay, J.L. (2007). Neuromechanics of muscle synergies for posture and movement. *Curr. Opin. Neurobiol.* *17*, 622–628.
- Tohyama, M., Sakai, K., Salvetti, D., Touret, M., and Juvet, M. (1979). Spinal projections from the lower brain stem in the cat as demonstrated by the horseradish peroxidase technique. I. Origins of the reticulospinal tracts and their funicular trajectories. *Brain Res.* *173*, 383–403.
- Uchino, Y., Sasaki, M., Sato, H., Bai, R., and Kawamoto, E. (2005). Otolith and canal integration on single vestibular neurons in cats. *Exp. Brain Res.* *164*, 271–285.
- Wilkinson, K.A., Maurer, A.P., Sadacca, B.F., and Yates, B.J. (2004). Responses of feline medial medullary reticular formation neurons with projections to the C5–C6 ventral horn to vestibular stimulation. *Brain Res.* *1018*, 247–256.
- Wilson, V.J., and Melville Jones, G. (1979). *Mammalian Vestibular Physiology* (Plenum Press).
- Wilson, V.J., and Peterson, B.W. (1978). Peripheral and central substrates of vestibulospinal reflexes. *Physiol. Rev.* *58*, 80–105.
- Wilson, V.J., and Yoshida, M. (1968). Vestibulospinal and reticulospinal effects on hindlimb, forelimb, and neck alpha motoneurons of the cat. *Proc. Natl. Acad. Sci. USA* *60*, 836–840.
- Wilson, V.J., and Yoshida, M. (1969). Comparison of effects of stimulation of Deiters' nucleus and medial longitudinal fasciculus on neck, forelimb, and hindlimb motoneurons. *J. Neurophysiol.* *32*, 743–758.
- Witts, E.C., Zagoraiou, L., and Miles, G.B. (2014). Anatomy and function of cholinergic C bouton inputs to motor neurons. *J. Anat.* *224*, 52–60.
- Zagoraiou, L., Akay, T., Martin, J.F., Brownstone, R.M., Jessell, T.M., and Miles, G.B. (2009). A cluster of cholinergic premotor interneurons modulates mouse locomotor activity. *Neuron* *64*, 645–662.
- Zampieri, N., Jessell, T.M., and Murray, A.J. (2014). Mapping sensory circuits by anterograde transsynaptic transfer of recombinant rabies virus. *Neuron* *81*, 766–778.
- Zhong, G., Droho, S., Crone, S.A., Dietz, S., Kwan, A.C., Webb, W.W., Sharma, K., and Harris-Warrick, R.M. (2010). Electrophysiological characterization of V2a interneurons and their locomotor-related activity in the neonatal mouse spinal cord. *J. Neurosci.* *30*, 170–182.